İSTANBUL UNIVERSITY CERRAHPAŞA

ORIGINAL ARTICLE
Electrica 2022; 22(1): 92-100

Design and Analysis of Printed Monopole Antenna With and Without CSRR in the Ground Plane for GSM 900 and Wi-Fi

Prasanna G. Paga[1], H. C. Nagaraj[1], K. S. Shashidhara[1], Veerendra Dakulagi[2], Kim Ho Yeap[3]

[1]Department of Electronics and Communication Engineering, Nitte Meenakshi Institute of Technology, Bangalore, India
[2]Department of Electronics and Communication Engineering, Guru Nanak Dev Engineering College, Bidar, Karnataka, India
[3]Faculty of Engineering and Green Technology, Universiti Tunku Abdul Rahman, Kampar, Malaysia

Cite this article as: P. G. Paga, H. C. Nagaraj, K. S. Shashidhara, V. Dakulagi, K. H. Yeap, "Design and Analysis of Printed Monopole Antenna with and without CSRR in the Ground Plane for GSM 900 and Wi-Fi," *Electrica*, 22(1), 92-100, Jan. 2022.

ABSTRACT

A dual-band printed monopole antenna with and without complementary split-ring resonator (CSRR) has been designed on an FR4 substrate of permittivity 4.4 and thickness 1.6 mm with a line feeding technique that finds application in GSM 900 and Wi-Fi. Two conducting strips were used to tune to 0.9 GHz and 2.4 GHz. The reflection coefficient values reported were −19.8 dB at GSM 900 and −6.4 dB at Wi-Fi. The novelty of the proposed work lies in using two concentric circular split rings etched beneath the antenna on the ground plane with a suitable gap g1 and g2. The outer ring was tuned to GSM 900 and the inner ring was tuned to Wi-Fi. By suitably adjusting the gap widths g1 and g2 and the ring thickness, the simulated value of the reflection coefficient showed a considerable improvement of −25.32 dB and −12.07 dB along with a gain of 6.17 dBi and 7.286 dBi in the lower- and the upper-frequency bands, respectively. The antenna dimensions were 100 mm × 40 mm × 1.6 mm.
***Index Terms*—**Antenna, CSRR, GSM 900, Wi-Fi

I. INTRODUCTION

Monopole antennas have gained widespread importance in day-to-day communication applications due to their small size and low profile nature due to which they are used frequently in wireless communication applications. Today's wireless communication devices such as mobile phones and laptops incorporate antennas that are tuned to single-frequency bands of interest. With the explosive growth of the wireless communication standards, more antennas need to be integrated into a device increasing its complexity. Dual and multi-band antennas give a promising solution to this problem as a single antenna can serve to tune two or more frequency bands of interest thereby resulting in the optimization of the space required in these devices. Yousfi et al. [1] proposed an inverted L-shaped antenna at 2.45 GHz and 5.8 GHz, respectively, for radio-frequency identification (RFID) applications.

The dual-band characteristics were achieved by etching the complementary split-ring resonator (CSRR) in the ground plane. The bandwidths reported were 0.4 GHz and 1.6 GHz for lower- and higher-frequency bands, respectively. The reported gains were 1.76 dBi and 5.75 dBi across both the frequency bands, respectively. Purushothaman et al. [2] proposed the design of a compact metamaterial-inspired antenna for L/S band applications. Defected ground plane structures were being used for getting the dual-band operation. The maximum gain variations were from 2.0 dBi to 2.3 dBi across both the frequency bands. Yue et al. [3] proposed a novel compact dual-band dual-polarized antennas with CSRR loading in the ground plane. The structure reported a resonant frequency of 1.95 GHz and 2.45 GHz with an input reflection coefficient of −20 dB and −40 dB at both the lower- and the upper-frequency bands, respectively. The structure was designed on a Rogers R003 substrate of permittivity 3 and loss tangent 0.0014 with a thickness of 1.5 mm. The peak gain reported was 6.0 dBi at both the frequency bands of interest. Sarkar et al. [4] investigated a compact dual-band four-element multiple input multiple output (MIMO) antenna array for pattern diversity. The radiating structure was designed to resonate at 1.9 GHz and 2.5 GHz for long-term evolution (LTE), global system for mobile communications (GSM), and wireless local area network (WLAN) applications. The structure was designed on an

Corresponding Author:
Veerendra Dakulagi

E-mail:
veerendra.gndec@gmail.com

Received: July 2, 2021

Accepted: August 23, 2021

Available Online Date: September 27, 2021

DOI: 10.5152/electrica.2021.21080

FR4 substrate using an L-shaped strip with CSRR to achieve the dual-band operation.

The peak gain reported was 3 dBi across both the frequency bands of interest. Atolia and Yadav [5] proposed a CSRR-loaded rectangular monopole antenna for ultra-wideband (UWB) applications. The UWB characteristics were achieved with the help of two CSRR-loaded slots near the feeding structure. The structure showed a good impedance matching from 3.4 GHz to 13.6 GHz, where the reflection coefficient was below −10 dB. The structure was designed on an FR4 substrate of permittivity 4.4 and thickness 1.6 mm. The size of the structure reported was 32 mm × 36 mm. Kareem et al. [6] designed a single parasitic split-ring resonator with an umbrella-shaped patch on the top of the substrate. The structure showed a good impedance match from 3.3 GHz to 4.58 GHz and from 5.1 GHz to 5.6 GHz wherein the input reflection coefficient remained below −10 dB. The gain reported was stable with a peak value of 5.5 dBi. The radiating structure was designed on an FR4 substrate of permittivity of 4.4 and thickness 1.6 mm. Yue et al. [7] proposed a miniaturized dual-band dual circularly polarized metasurface antenna. The radiating structure showed resonances at 1.87 GHz and 2.48 GHz wherein the input reflection coefficient remained well below −10 dB. The peak gains reported were 3.95 dBi and 5.29 dBi along with a bandwidth of 50 MHz for both the lower- and the upper-frequency bands, respectively. The structure was designed on a Rogers RO 4003C substrate of permittivity 3.55 with a size of 0.33λ0 × 0.33λ0.

Bapat et al. [8] proposed the design of a UWB antenna with dual-band rejection characteristics using shorted CSRRs. The shorted CSRR was used to reject 5.5 GHz and 3.5 GHz frequencies from the UWB frequency range of 3.1 GHz–10.5 GHz. Li et al. [9] designed a planar antenna using transmission line-based metamaterial loading for 3G/Bluetooth and Wi-Max applications. The dual notch characteristics were obtained from 5 GHz to 5.5 GHz and from 7.2 GHz to 7.6 GHz frequency bands of interest wherein the *S*11 remained below −10 dB. Manage et al. [10] presented a dual band-notched UWB MIMO antenna by incorporating CSRR for WLAN and X band applications. The dual-band characteristics were achieved by etching J- and L-shaped slots with CSRR. The structure was designed on an FR4 substrate with a size of 18 mm × 30 mm × 1.6 mm.

Li et al. [11] designed an UWB antenna using CSRR and SRR that finds applications in automotive communications. The CSRRs were designed for achieving dual-band characteristics, and the SRRs were primarily used for improving the isolation characteristics between the two antenna elements. The overall dimensions of the antenna structure were 54 mm × 33 mm. The UWB characteristics were obtained from 3 GHz to 12 GHz with a peak gain variation in the range of 0 dBi–5 dBi at 3.2 GHz, 6.5 GHz, and 10 GHz frequency bands of interest. Sethi et al. [12] designed a conventional coplanar waveguide (CPW)-fed MIMO antenna for UWB applications. The antenna is printed on a polyethylene terephthalate (PET) substrate using silver nanoparticle ink. An inverted U-shaped notch has been printed on the antenna with four ports resulting in a 4 × 4 MIMO antenna array. The input reflection coefficient was well below −10 dB over the operating band from 3.1 GHz to 11.1 GHz frequency range of interest. The error correction code (ECC) value reported was in the range of 0.002–0.003 with a peak diversity gain of 9.98 dB at 8 GHz frequency.

Wang et al. [13] designed a polarization diversity UWB antenna on an FR4 substrate of permittivity 4.4 and thickness 1.6 mm with a relative permittivity of 4.55. The size of the structure reported was 24 mm × 44 × 0.8 mm. The polarization diversity was obtained by aligning the antennas with an angle of 90°. An inverted L-shaped strip was printed on the ground plane for size reduction and improving the impedance bandwidth. Huang et al. [14] designed a compact MIMO antenna with a controllable bandwidth. The antenna size reported was 32 mm × 26 mm × 0.8 mm printed on an FR4 substrate of permittivity 4.4. The radiating structure reported an input reflection coefficient which was well below −10 dB over the operating band of the antenna extending from 3 GHz to 12 GHz. The S12 value reported was −15 dB in the frequency band of interest.

Li et al. [15] designed a UWB MIMO antenna using a slot and a stub technique. Two identical semi-circle ring-shaped UWB monopole antennas were designed and placed side by side. By incorporating two L-shaped slots on the ground plane, dual notch characteristics were realized. The anchor-shaped stubs were also printed to suppress the interference signal. The proposed structure resulted in very high isolation of −19.74 dB across the UWB band. Suhane et al. [16] designed a diversity antenna using the MIMO technique for UWB applications. The antenna was designed on an FR4 substrate of relative permittivity 4.4. The band notch characteristics were observed by introducing two inverted L-shaped slits inside the patch. The radiating structure showed good isolation of −20 dB with an envelope correlation coefficient value below 0.1 over the entire band of 2.5 GHz–10 GHz. The peak gain reported was 4.8 dBi. Manage et al. [17] investigated a dual band-notched UWB MIMO antenna incorporating circular split ring resonators in the ground plane, which finds applications for WLAN. Two closely spaced monopole antennas under MIMO configurations were designed to tune to 8.2 GHz and 5.2 GHz. The designed antenna showed good isolation characteristics well below −23 dB over the operating frequency range from 3.1 GHz to 12 GHz. The diversity gain variations were in the range from 9.97 to 10.

Quddus et al. [18] proposed a two-port diversity MIMO antenna with dual notch characteristics for UWB applications. Dual notch characteristics were observed by printing U-shaped slots on the main radiator and horizontal stubs in the ground plane. The envelope correlation coefficients were in the range of 0.1–0.25 over the entire UWB band. Shehata et al. [19] designed a MIMO antenna element with interference suppression for UWB applications. The antenna elements have been designed on an FR4 substrate of thickness 1.6 mm and occupy an area of 100 mm × 100 mm. The antenna achieved the isolation of over 20 dB with band notches at 3.5 GHz and 5.5 GHz with an envelope correlation coefficient below 1.0.

II. PROPOSED SYSTEM

In the proposed work, a dual-band antenna has been designed on an FR4 substrate of permittivity 4.4 and thickness 1.6 mm to tune between GSM 900 and the Wi-Fi (2.4 GHz) frequency band. The antenna has two radiating strips supported on a partial ground plane to give a monopole-like feature. The longer conductor of length L1 is designed to resonate at GSM 900 frequency band that is at 0.9 GHz while the shorter strip of length L2 is tuned to resonate at

TABLE I. GEOMETRICAL SPECIFICATIONS OF THE ANTENNA

Antenna Dimensions	Optimized Value
Length of the substrate, L_s	100 mm
Width of the substrate, W_s	40 mm
Ground plane length, $L_g = 6h + L_{2.4}$	11.5 mm
Ground plane width, $W_g = 6h + W_{2.4}$	40.0 mm
Feed width	3 mm
Length of the monopole for 0.9 GHz, $L1$	76.9 mm
Length of the monopole for 2.4 GHz, $L2$	32.9 mm
Diameter of outer circular split ring ($D1$)	26 mm
Gap width, $g1$	2 mm
Diameter of the inner circular split ring ($D2$)	14 mm
Gap width, $g2$	1 mm

the 2.4 GHz frequency band of interest. The dimensions of both the strips have been calculated corresponding to quarter wavelength resonance condition for GSM 900 and Wi-Fi. To improve the reflection coefficient of the antenna, two circular split rings have been printed on the ground plane. The diameter of the outer split ring has been kept at 26 mm, and the total circumference of the outer split ring has been made equal to $\lambda g/2$, where λg corresponds to guide wavelength corresponding to GSM 900 frequency band of interest. The diameter of the inner split ring has been kept at 14 mm to tune to the Wi-Fi frequency band of interest. The length of the split rings gives an inductive effect while the gap between the rings provides a capacitative effect.

The geometrical specifications of the antenna are tabulated in Table I.

III. ANTENNA DESIGN CONSIDERATIONS

In this work, a dual-band monopole antenna has been designed using circular split ring resonator in the ground plane. The length of the longer strip $L1$ has been kept at quarter of guide wavelength corresponding to GSM 900 frequency band of interest, and the length of the shorter strip $L2$ has been kept at quarter of guide wavelength corresponding to Wi-Fi 2.4 GHz frequency bands of interest as shown in Fig. 1(a). Partial ground plane structure has been selected to give it a monopole design. Two circular split rings have been printed beneath the antenna sharing a common center. The circumference of the outer split ring has been kept at half the guide wavelength corresponding to GSM 900.A small gap $g1$ has been added to fine tune the ring in the GSM 900 frequency band. The circumference of the inner ring has been kept at a value equal to half the guide wavelength corresponding to Wi-Fi frequency band as shown in Fig. 1(b). A small slot in the form of gap $g2$ has been printed on the inner ring so as to cause additional tuning in the Wi-Fi band. The ring thickness of outer ring and the inner rings have been appropriately varied and optimized to cause dual band operation. The fabricated prototype model of the antenna is as shown in Fig. 2(a), while the ground plane view with CSRR is reported in Fig. 2(b).

$$L1 = \lambda g / 4 \tag{1}$$

$$\lambda_g = \lambda_0 / \sqrt{\varepsilon_{reff}} \tag{2}$$

where $L1$ is the length of monopole section at GSM 900 band, λ_g is the guide wavelength corresponding to GSM 900 frequency band of interest, λ_0 is the free space wavelength, and ε_{reff} is the effective permittivity of the substrate.

$$\varepsilon_{reff} = \left[\left(\frac{\varepsilon_r + 1}{2} \right) + \left(\frac{\varepsilon_r - 1}{2} \right) \left(1 + 12 \frac{h}{w} \right)^{\frac{-1}{2}} \right] \tag{3}$$

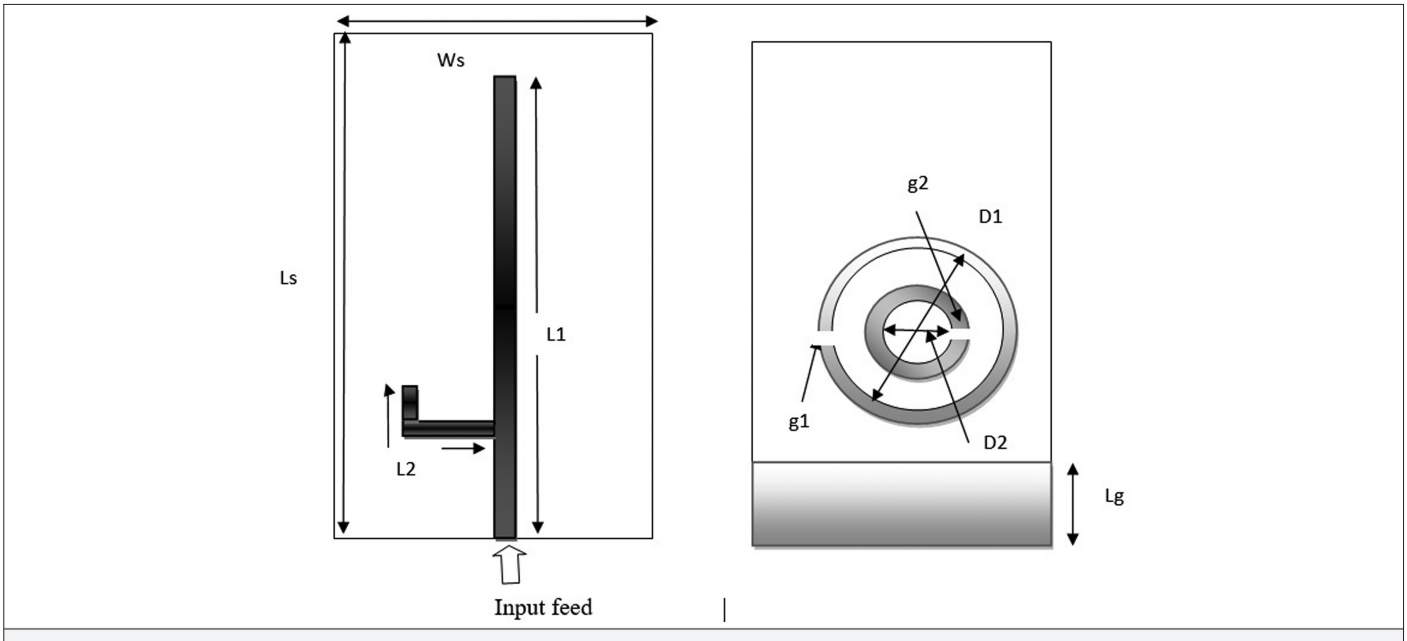

Fig. 1. (a) Top view of the simulated antenna structure and (b) structure of CSRR.

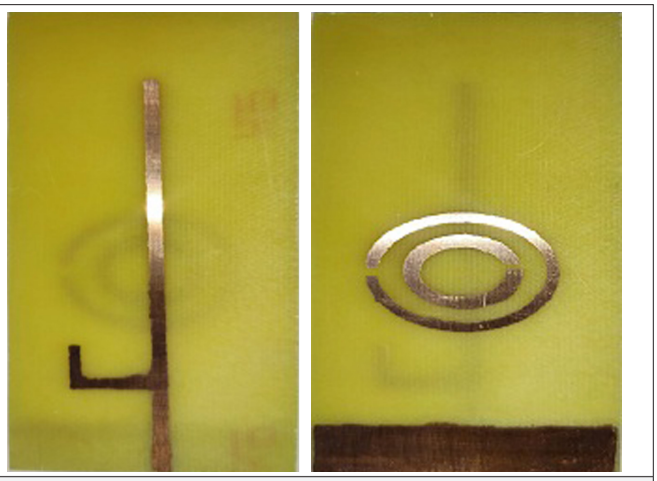

Fig. 2. (a) Top view of the fabricated dual-band monopole antenna. (b) Ground plane view of the antenna with CSRR.

where w is the width of the antenna and h is the thickness of the substrate.

$$L2 = \lambda_g / 4 \tag{4}$$

where $L2$ is the length of the shorter section radiating at 2.4 GHz frequency, λ_g is the guide wavelength corresponding to Wi-Fi.

$$C1 = \text{circumference of outer split ring} = \pi D1 = \lambda g1 / 2 - g1 \tag{5}$$

where $\lambda g1$ is the guide wavelength corresponding to GSM 900 and $g1$ is the gap width of outer ring.

$$C2 = \text{circumference of inner split ring} = \pi D2 = \lambda g2 / 2 - g2 \tag{6}$$

where $\lambda g2$ is the guide wavelength corresponding to 2.4 GHz and $g2$ is the gap width of inner ring.

$$z = \frac{60}{\varepsilon reff} \ln\left(\frac{8h}{wf} + \frac{wf}{4h}\right) \tag{7}$$

where $Z = Z0 =$ characteristic impedance of the line $= 50\ \Omega$, h is the substrate thickness, and wf is the feed width

IV. DESIGN METHODOLOGY

1. Select the resonant frequencies, substrate type, and permittivity
2. Compute the length of the antenna $L1$ at GSM 900 under quarter wavelength resonance condition using (1).
3. Compute the length of the antenna $L2$ at Wi-Fi 2.4 GHz under quarter wavelength resonance condition using (4)
4. Compute the effective permittivity and feed width (wf) for getting 50 Ω impedance matching using (3) and (7).
5. Connect the two strips perpendicular to each other such that the current density is maximum at that point and etch a partial ground plane beneath the patch.
6. Create a 3D model of the antenna in HFSS and assign boundaries and excitations.
7. Create a solution setup corresponding to the GSM 900 and Wi-Fi (2.4 GHz) frequency band of interest and assign frequency sweep for both the setups.
8. Perform a validation check and compute the $S11$ and check if it is below −10 dB at both the designated frequencies, else optimize the antenna dimensions.
9. Print two concentric circular split-ring resonators in the ground plane beneath the center of the longer strip such that both the centers share a common centroid.
10. Select the circumferences of both the split rings to be equal to half of the guide wavelength with appropriate thickness and gap widths $g1$ and $g2$ corresponding to GSM 900 and Wi-Fi 2.4 GHz, respectively.
11. Optimize the ring thickness and the gap widths $g1$ and $g2$ such that the input reflection coefficient comes below −10 dB at both the frequency bands of interest.
12. Fabricate the antenna on an FR4 substrate of thickness 1.6 mm.

V. SIMULATED RESULTS

The simulation of the antenna has been carried out in Ansoft HFSS version 15.0, and the results have been tabulated as shown.

The $S11$ values reported were −25.32 dB and −12.07 dB at GSM and Wi-Fi frequency bands, respectively. The −10 dB impedance bandwidth was extending from 0.92 GHz to 0.99 GHz for the GSM band. For the Wi-Fi band, the corresponding values were extending from 2.09 GHz to 2.45 GHz.

The input reflection coefficient values reported were −19.8 dB and −6.4 dB at GSM and Wi-Fi frequency bands, respectively. The −10 dB impedance bandwidth was extending from 0.97 GHz to 1.0656 GHz giving a total of 92 MHz in the lower band. While in the upper band at 2.4 GHz, the bandwidth reported is zero.

The CSRR has the effect of lowering the input reflection coefficient value both in the GSM 900 and Wi-Fi frequency band of interest as compared to that without CSRR.

The ground plane has the effect of lowering the input reflection coefficient, and the curve has shifted toward the right indicating an improvement in the −10 dB impedance bandwidth.

As the outer ring thickness is varied from 1 mm to 4 mm, the input reflection coefficient has decreased from −12 dB to −25 dB at 2.4 GHz frequency band of interest.

As the thickness of the ring increases, the input reflection coefficient curve shifts slightly upward.

As the gap width $g2$ decreases, the input reflection coefficient curve shifts upward for both the frequency bands of interest.

The gap width $g2$ has the effect of shifting the input reflection coefficient curve toward the right and controls the bandwidth in the upper band.

The peak gain reported was 6.32 dBi under both the E and H planes at the GSM 900 frequency band of interest.

The peak gain reported was 6.17 dBi at GSM 900 band under both E and H planes. The corresponding value in the Wi-Fi band was 7.286 dBi.The horizontal axis represents the phase angle in degree, while the vertical axis represents the gain (in dBi).

The current essentially is concentrated on the longer conducting strip resonating at 0.9 GHz with a maximum density equal to 84.72 A/m coming out from the longer conducting strip *L*1 inferring that the radiation essentially takes place through *L*1 at the GSM 900 frequency band of interest.

The magnitude of the surface current density reported was 80.199 A/m. The current density is mainly concentrated near the shorter conducting strip inferring that the radiation is dominated by shorter conducting strip *L*2.

VI. RESULTS AND DISCUSSIONS

The antenna results have been neatly tabulated and presented in Table II, and the geometrical specifications of the antennas have been reported in Table I. The simulated *S*11 values with CSRR as reported in Fig. 3 were −25.32 dB and −12.07 dB in the lower- and the upper-frequency bands, respectively, as against −19.8 dB (GSM 900) and −6.4 dB (Wi-Fi) without CSRR as reported in Fig. 4. There is a significant increase in the reflection coefficient of about 5.52 dB in the lower band and 5.67 dB in the upper band, respectively, as represented in Fig. 5. The corresponding bandwidths reported were 0.075 GHz and 0.360 GHz across both the GSM 900 and Wi-Fi bands with CSRR. However, without CSRR, the corresponding value reported was 0.092 GHz in the lower GSM band as reported in Table II.

TABLE II. COMPARISON OF THE ANTENNA PERFORMANCE PARAMETERS WITH AND WITHOUT CSRR

Antenna Parameter	Simulated Results With CSRR		Simulated Results Without CSRR	
	GSM 900	Wi-Fi	GSM 900	WI-FI
Return loss	−25.32 dB	−12.07 dB	−19.8 dB	−6.4 dB
Bandwidth	0.075 GHz	0.360 GHz	0.092 GHz	0
Gain	6.17 dBi	7.286 dBi	6.32 dBi	------

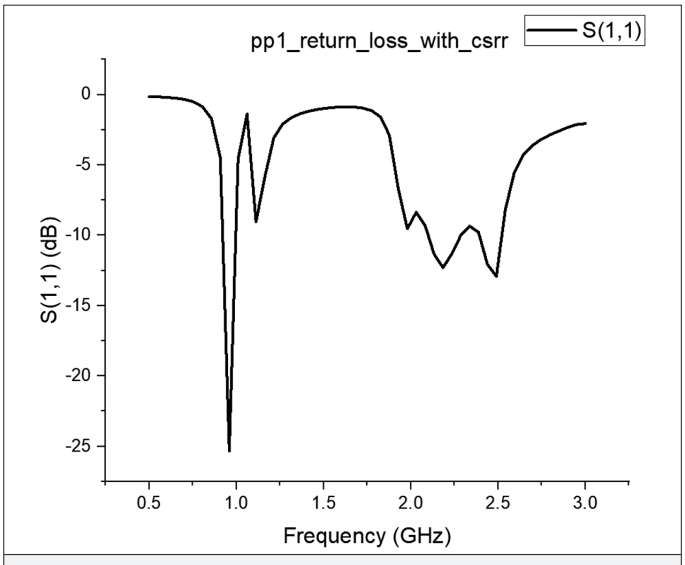

Fig. 3. Simulated *S*11 plot of the antenna at 0.9 GHz and 2.4 GHz with CSRR.

A parametric analysis was done on the antenna structure by varying the ground plane, ring thickness, and the gap widths of the circular split ring. As the ground plane length was varied from 11.2 mm to 11.8 mm, the simulated input reflection coefficient decreased from −12.5 dB to −17.5 dB as reported in Fig. 6. The ground plane has the effect of lowering the input reflection coefficient in the 2.4 GHz frequency band, and the curve has shifted toward the right indicating an improvement in the −10 dB impedance bandwidth.

As the outer ring thickness is varied from 1 mm to 4 mm, the input reflection coefficient decreased from −12.0 dB to −25 dB at 2.4 GHz frequency band of interest. However, in the GSM 900 band, the input reflection coefficient reported a maximum value of −28 dB when the ring thickness was 2 mm as reported in Fig. 7**.** As the thickness of the inner ring increases, the input reflection coefficient curve shifts downward in the Wi-Fi band. The input reflection coefficient changed from −12.5 dB to −25 dB as reported in Fig. 8.

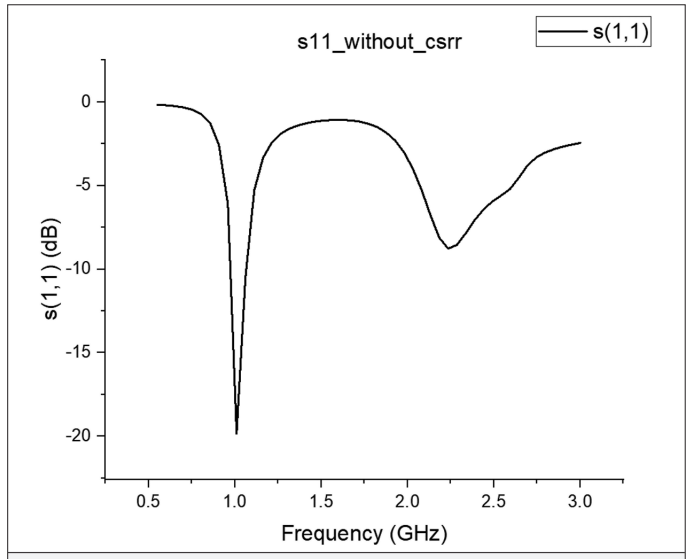

Fig. 4. Simulated *S*11 plot of the antenna without CSRR.

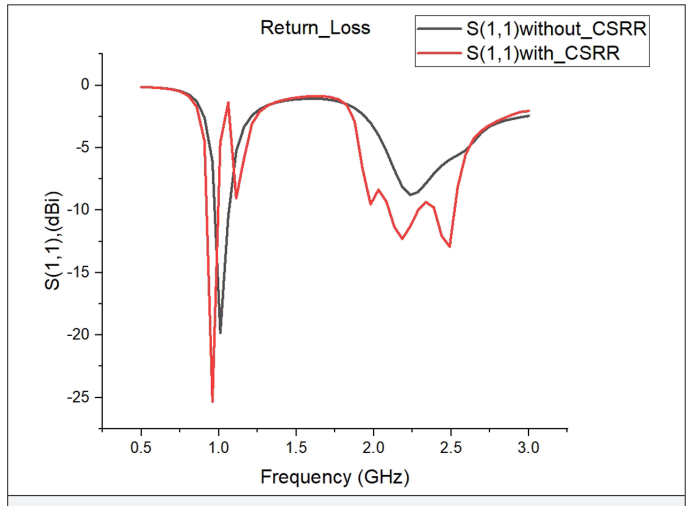

Fig. 5. Simulated return loss plot of the radiating structure considering with and without CSRR.

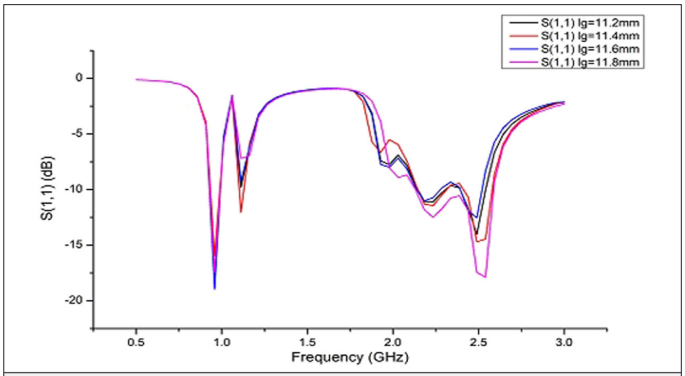

Fig. 6. Simulated *S*11 plot of the antenna showing the effect of varying the ground plane length from 11.2 mm to 11.8 mm.

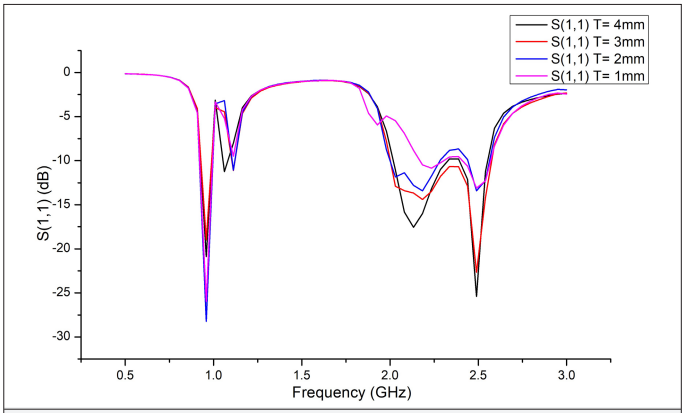

Fig. 7. Simulated *S*11 plot of the antenna showing the effect of varying the ring thickness of the outer ring.

As the gap width *g*2 decreases, the input reflection coefficient curve shifts upward creating poor resonance at the Wi-Fi band as shown in Fig. 9. The best results were obtained when the inner gap width was kept at 0.3 mm wherein the *S*11 values reported were −25 dB and −18 dB at the GSM 900 and Wi-Fi frequency bands, respectively.

As the gap width *g*1 of the outer split ring decreases, the input reflection coefficient in the GSM 900 band varied from −25 dB to −20 dB as reported in Fig. 10. In the Wi-Fi band, the bandwidth became narrow

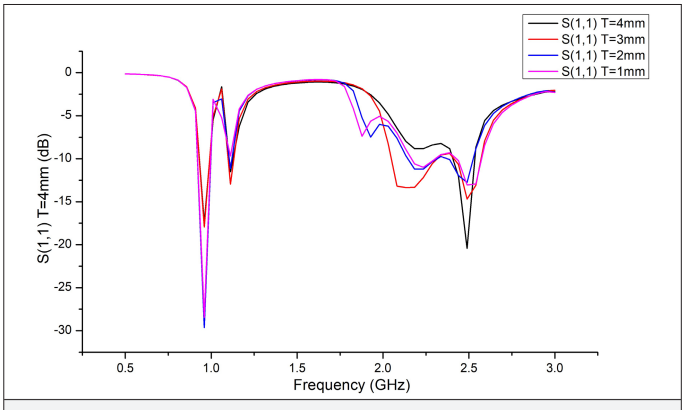

Fig. 8. Simulated *S*11 plot of the antenna showing the effect of varying the inner split ring thickness.

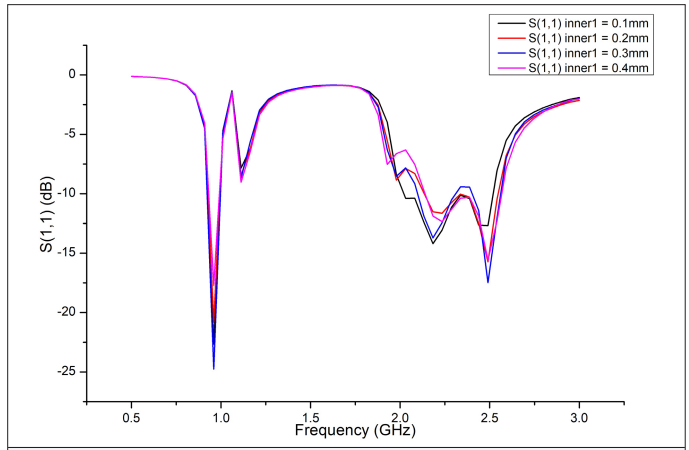

Fig. 9. Simulated *S*11 plot of the antenna showing the effect of varying the gap width *g*2 of inner split ring from 0.1 mm to 0.4 mm.

thereby lowering the bandwidth. The gap width *g*1 has the effect of controlling the input reflection coefficient in the GSM 900 band.

The radiation pattern reported was relatively Omni-directional under both the E and H planes with a peak bore sight gain of 6.32 dBi in the GSM 900 frequency band of interest without CSRR as reported in Fig. 11. However, with CSRR, the corresponding peak gains reported were 6.17 dBi and 7.286 dBi at both the lower- and the upper-frequency bands, respectively as reported in Fig. 12.

The simulated surface current density plot of the antenna has been shown in Fig. 13 corresponding to the GSM 900 frequency band of interest. As seen, the current density is concentrated on the surface of the longer conducting strip with a peak value of 84.72A/m^2. In the Wi-Fi band, the current density essentially remains on the shorter conducting strip *L*2 with a peak value of 80.199 A/m^2 as reported in Fig. 14.

The reflection coefficient reported was −25.32 dB, which is reasonably good compared to other works reported in the literature, in the lower frequency bands of interest as reported in Table III. The peak gains reported were also relatively higher when compared to [2,4] wherein the peak gain variation was in the range of 2.0 dBi–3.0 dBi. The bandwidth reported was comparatively higher at the lower

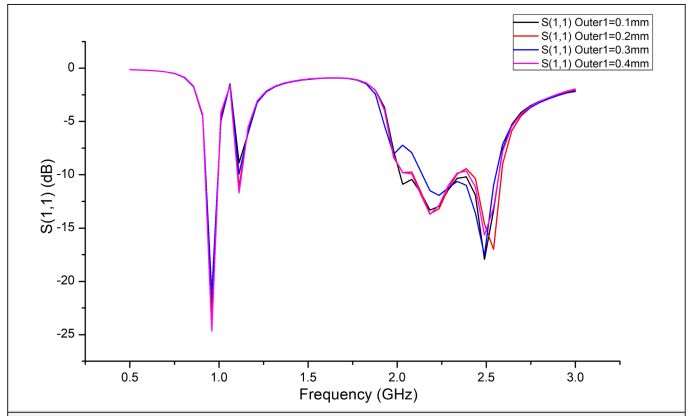

Fig. 10. Simulated *S*11 plot of the antenna showing the effect of varying the outer gap width *g*1 of the outer split ring from 0.1 mm to 0.4 mm.

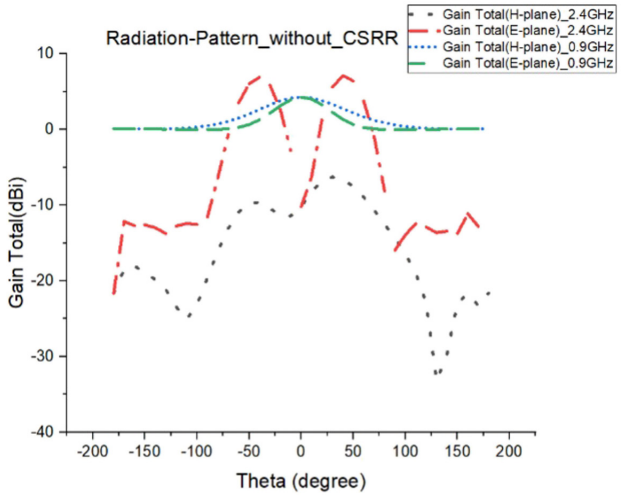

Fig. 11. Simulated radiation pattern of the antenna at GSM 900 and Wi-Fi without CSRR.

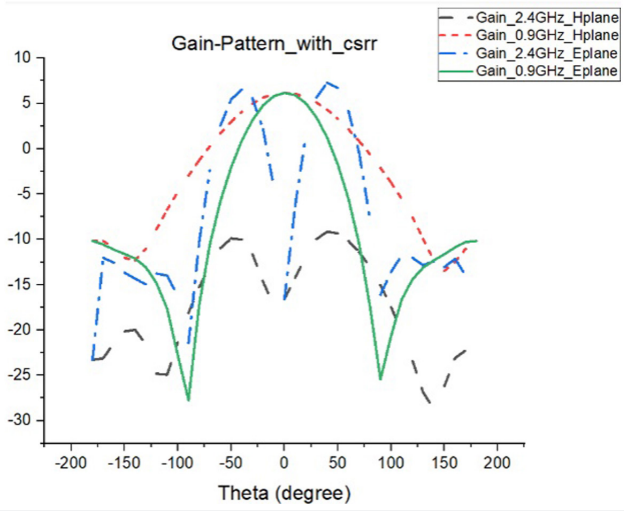

Fig. 12. Simulated radiation pattern of the antenna at GSM 900 and Wi-Fi with CSRR.

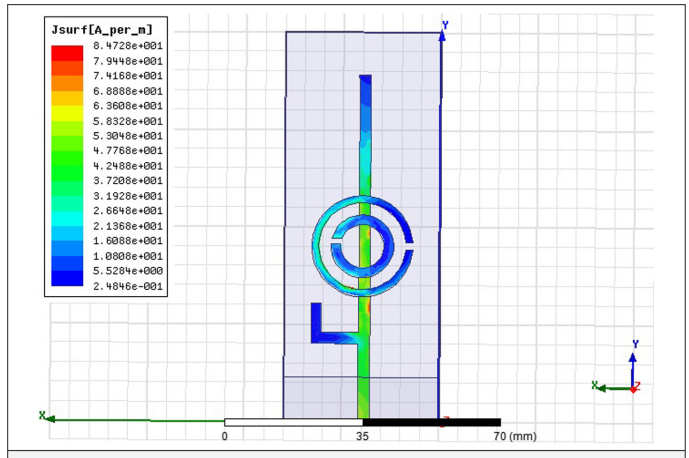

Fig. 13. Surface current density plot of the antenna resonating at 0.9 GHz.

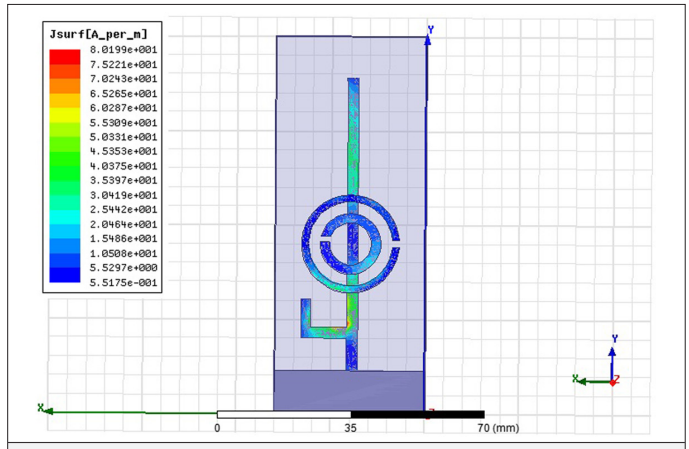

Fig. 14. Surface current density plot of the antenna resonating at 0.9 GHz.

TABLE III. COMPARISON OF THE PRESENT WORK WITH SIMILAR OTHER WORKS REPORTED IN THE LITERATURE

Antenna Parameters	Present Work	[2]	[4]	[7]
Resonant frequency	0.9 GHz and 2.4 GHz	1.154 GHz and 2.497 GHz	1.9 GHz and 2.5 GHz LTE,GSM, and WLAN	1.87 GHz and 2.48 GHz
Return loss	−25.32 dB and −12.07 dB	−25 dB and −28 dB	−13 dB and −20 dB	−22.0 dB and −12.0 dB
Gain	6.17 dBi and 7.286 dBi	2.0 dBi–3.0 dBi	3.0 dBi	3.95 dBi–5.29 dBi
Bandwidth	75 MHz and 360.4 MHz	126 MHz and 55 MHz	235 MHz and 364 MHz	50 MHz
Antenna parameters	Present work	[2]	[4]	[7]
Resonant frequency	0.9 GHz and 2.4 GHz	1.154 GHz and 2.497 GHz	1.9 GHz and 2.5 GHz LTE,GSM, and WLAN	1.87 GHz and 2.48 GHz
Return loss	−25.32 dB and −12.07 dB	−25 dB and −28 dB	−13 dB and −20 dB	−22.0 dB and −12.0 dB
Gain	6.17 dBi and 7.286 dBi	2.0d Bi–3.0 dBi	3.0 dBi	3.95 dBi–5.29 dBi
Bandwidth	75 MHz and 360.4 MHz	126 MHz and 55 MHz	235 MHz and 364 MHz	50 MHz

band when compared to [7]. However, at the Wi-Fi band, the corresponding values were much greater as reported in [2,7].

VII. CONCLUSION

In this work, a dual-band monopole antenna with two concentric split ring resonators has been designed and analyzed at GSM 900 and Wi-Fi frequency bands of interest. The simulated *S*11 values were −19.8 dB and −6.4 dB without CSRR in the ground plane. The dual-band monopole antennas had shown very poor reflection coefficient characteristics in the Wi-Fi Frequency band of interest wherein the value reported was −6.4 dB as reported in Table II. Subsequently etching two concentric circular split rings in the ground plane, and optimizing the ring thickness and the gap widths *g*1 and *g*2 of the two split rings, the input reflection coefficient values improved to −25.32 dB and −12.07 dB at the lower GSM 900 and Wi-Fi frequency bands of interest. The circular split ring resonator has the effect of improving the *S*11 by a factor −5.32 dB in the GSM 900 and −5.67 dB in the Wi-Fi band along with a bandwidth improvement of 360 MHz in the Wi-Fi band as reported in Table II.

VIII. FUTURE SCOPE

The circular split ring resonators have the potential of improving the performance parameters of the antenna if properly placed on the ground plane. They also help in the miniaturization of the antenna structure. By varying the ring thickness and the gap between the rings, additional tuning of the antenna can be realized. Different modifications in ring structures such as square, hexagonal can also be investigated to improve the antenna performance. Metamaterial loading with spiral electromagnetic band gap structures can also be investigated to improve the reflection coefficient and the gain while reducing the antenna size.

Peer-review: Externally peer-reviewed.

Author Contributions: Concept - P.G.P., H.C.N., K.S.S., V.D., K.H.Y.; Design - P.G.P., H.C.N., K.S.S., V.D., K.H.Y.; Supervision - P.G.P., H.C.N., K.S.S., V.D., K.H.Y.; Resources - P.G.P., H.C.N., K.S.S., V.D., K.H.Y.; Materials - P.G.P., H.C.N., K.S.S., V.D., K.H.Y.; Data Collection and/or Processing - P.G.P., H.C.N., K.S.S., V.D., K.H.Y.; Analysis and/or Interpretation - P.G.P., H.C.N., K.S.S., V.D., K.H.Y.; Literature Search - P.G.P., H.C.N., K.S.S., V.D., K.H.Y.; Writing Manuscript - P.G.P., H.C.N., K.S.S., V.D., K.H.Y.; Critical Review - P.G.P., H.C.N., K.S.S., V.D., K.H.Y.

Conflict of Interest: The authors have no conflicts of interest to declare.

Financial Disclosure: The authors declared that this study has received no financial support.

REFERENCES

1. E. Yousfi, A. Es-Salhi, A. Lamkaddem, O. El Mrabet, M. Aznabet and M. Ali Ennasar, "A dual band inverted L monopole antenna based on complemenatry split ring resonator for RFID applications," in *2019 International Conference on Wireless Technologies, Embedded and Intelligent Systems (WITS)*, Fez, Morocco, 2019, pp. 1–3. [CrossRef]
2. S. Purushothaman, S. Raghavan and V. S. Kumar, "A design of compact metamaterial encumbered monopole antenna with defected ground structure for navigation (L/S-band) applications," in *2016, IEEE Annual India Conference (INDICON)*, Bangalore, India, 2016, pp. 1–4. [CrossRef]
3. T. Yue and D. H. Werner, "Compact dual-band dual-polarized antenna enabled by a CSRR loaded metasurface," in *2017 IEEE International Symposium on Antennas and Propagation & USNC/URSI National Radio Sci. Meeting*, San Diego, CA, 2017, pp. 2471–2472. [CrossRef]
4. D. Sarkar, K. Saurav and K. V. Srivastava, "A compact four element CSRR-loaded antenna for dual band pattern diversity MIMO applications," in *46th Eur. Microwave Conference (EuMC)*, London, UK, 2016, pp. 1315–1318. [CrossRef]
5. D. Atolia and S. K. Yadav, "A rectangular monopole UWB patch antenna with CSRR slots having dual band notch characteristics," in *2017 IEEE International WIE Conference on Electrical and Computer Engineering (WIECON-ECE)*, Dehradun, 2017, pp. 108–112. [CrossRef]
6. B. A. Kareem, Z. A. A. Hassain and A. H. Sallomi, "Design of dual high band-notch UWB antenna based on CSRR and parasitic arms," in *2018 18th Mediterr. Microwave Symposium (MMS)*, Istanbul, Turkey, 2018, pp. 1–4. [CrossRef]
7. T. Yue, Z. H. Jiang and D. H. Werner, "A compact metasurface-enabled dual-band dual-circularly polarized antenna loaded with complementary split ring resonators," *IEEE Trans. Antennas Propag.*, vol. 67, no. 2, pp. 794–803, 2019. [CrossRef]
8. H. B. Bapat, V. N. Kamble and M. Tamrakar, "Dual band rejected UWB antenna using shorted CSRR," in *2019 International Conference on Vision Towards Emerging Trends in Communication and Networking (ViTECoN)*, Vellore, India, 2019, pp. 1–3. [CrossRef]
9. Wen Tao Li, Yong Qiang Hei, Wei Feng and Xiao Wei Shi, "Planar antenna for 3G/Bluetooth/WiMAX and UWB applications with dual band-notched characteristics," *IEEE Antennas Wirel. Propag. Lett.*, vol. 11, pp. 61–64, 2012. [CrossRef]
10. P. S. Manage, U. Naik, S. Kareemulla and V. Rayar, "Dual band notched UWB-MIMO antenna incorporating CSRR for WLAN and X Band applications," in *2020 Third International Conference on Smart Systems and Inventive Technology (ICSSIT)*, Tirunelveli, India, 2020, pp. 149–152. [CrossRef]
11. H. Li and Z. Jiang, "A CSRR and SRR based ultrawideband MIMO antenna with band-notched characteristics," in *2019 IEEE International Symposium on Antennas and Propagation and USNC-URSI Radio Sci. Meeting*, 2019, pp. 1137–1138. [CrossRef]
12. W. T. Sethi, K. Issa and S. A. Alshebeili, "An inkjet-printed UWB-MIMO antenna with band rejection capability for wireless network applications," in *2nd International Conference on Computer*, vol. 13, 2019
13. Y. Wang, F. Zhu and S. Gao, "Design of planar ultra-wideband antenna with polarization diversity and high isolation," in *2016 IEEE International Conference on Ubiquitous Wireless Broadband (ICUWB)*, 2016, pp. 1–3. [CrossRef]
14. H. Huang and S.-G. Xiao, "Compact dual-resonator loaded band-notched MIMO antenna with high frequency selectivity and controllable bandwidth," *Progress in Electromagnetic Research Symposium (PIERS)* vol. 2016, pp. 2742–2746, 2016. [CrossRef]
15. Y. Li, Y. Kong and K. Yu, "A dual band-notched UWB-MIMO antenna using slot and stub techniques," in 5th Asia Pac. Conference on Antennas and Propagation (APCAP). *IEEE Publications*, vol. 2016, pp. 313–314, 2016. [CrossRef]
16. S. suhane and P. K. Jain, "MIMO diversity antenna for UWB and WIMAX wireless applications," in *International Conference on Recent Trends on Electronics, Information and Communication Technology (RTEICT-2020)*, 2020, pp. 215–218. [CrossRef]
17. P. S. Manage, U. Naik, S. Kareemulla and V. Rayar, "Dual band notched UWB-MIMO antenna incorporating CSRR for WLAN and X Band applications," in *2020 Third International Conference on Smart Systems and Inventive Technology (ICSSIT)*, 2020, pp. 149–152. [CrossRef]
18. A. Quddus, R. Saleem, S. ur Rehman and M. F. Shafique, "Dual port UWB diversity/MIMO antenna with dual band-notch characteristics," in *2016 10th International Conference on Signal Processing and Communication Systems (ICSPCS)*, 2016, pp. 1–4. [CrossRef]
19. M. Shehata, M. S. Said and H. Mostafa, "Dual notched band quad-element MIMO antenna with multitone interference suppression for IR-UWB wireless applications," *IEEE Trans. Antennas Propag.*, vol. 66, no. 11, pp. 5737–5746, 2018. [CrossRef]

Prasanna Paga is currently working as an assistant professor in E&CE Department of Nitte Meenakshi Institute of Technology, Yelahanka, Bangalore. He completed his B.E. in electronics and communication engineering from PDA College of Engineering Gulbarga, M.Tech in industrial electronics from SJCE Mysore, and Ph.D. from University of Mysore on antennas. He has over 20 publications in reputed journals and conferences and has over 15 years of teaching experience.

H. C. Nagaraj is currently working as the Principal of Nitte Meenakshi Institute of Technology (NMIT), Bangalore. He holds a B.E. (Electronics and Communications) degree from the University of Mysore, an M.E. (Communication systems) degree from P.S.G. College of Technology, Coimbatore, and Ph.D. (Biomedical Signal Processing and Instrumentation) from Indian Institute of Technology, Chennai. He has teaching experience of almost four decades, Dr. H. C. Nagaraj aims to bring NMIT among the top 50 education institutes according to NIRF ranking. He has massive experience of 37 years in teaching. He has visited 15 countries and studied the University Engineering Education System, involving various laboratories, centers of excellence, and so on. He has published 30 papers nationally and internationally.

K. S. Shashidhara is currently working as an associate professor in E&CE Department of Nitte Meenakshi Institute of Technology, Yelahanka, Bangalore. He completed his B.E. in electronics and communication engineering from SJCE Mysore, M.Tech in industrial electronics from SJCE Mysore, and Ph.D. from Visveswaraya Technological University on Signal Processing for Communication. He has over 10 publications in reputed journals and conferences and has over 16 years of teaching experience.

Veerendra Dakulagi earned his B.E. in electronics and communication engineering and M.Tech. in power electronics from Visvesvaraya Technological University, Belagavi, India, in 2007 and 2011, respectively. He earned his Ph.D. degree in array signal processing from the same university in 2018. He worked as a lecturer in Sapthagiri Engineering College, Bangalore, India, from 2007 to 2008. Then he worked as an assistant professor in Bheemanna Khandre Institute of Technology, Bhalki, India, from 2009 to 2010. He worked as an assistant professor in department of electronics and communication engineering (E&CE) in Guru Nanak Dev Engineering College, Bidar, India, from 2010 to 2018. Currently, he is a dean (Research & Development) and an associate professor (E&CE) of the same institute. He has published over 30 refereed technical journals (including *IEEE Transactions*, *IEEE Journals*, *Elsevier*, *Springer*, and *Taylor & Francis*) and 1 patent in array signal processing. He has received many awards in education including, (1) the "Award for Research Publications" by vision group on science and technology, Govt. of Karnataka, India, under the leadership of Bharat Ratna Prof. C.N.R. Rao and (2) the best teacher/researcher award by Guru Nanak Dev Engineering College, Bidar, for the academic year 2018–2019. He is the editor in chief of (1) *Journal of Advanced Research in Wireless, Mobile & Telecommunication* and (2) *Journal of Advanced Research in Signal Processing & Applications*. Also, he serves as an associate editor for (1) *Journal of Communication Engineering and Systems* and (2) *Journal on Electronics Engineering*. He is a regular reviewer to various IEEE transactions/journals, Elsevier, Taylor & Francis, and Springer journals.

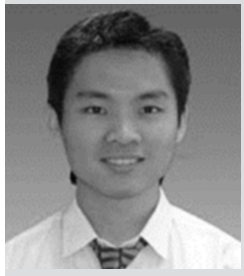

Kim Ho Yeap received his B.Eng. (Hons) from Universiti Teknologi Petronas in 2004, M.Sc. from Universiti Kebangsaan Malaysia in 2005, and Ph.D. from Universiti Tunku Abdul Rahman in 2011. In 2008 and 2015, he underwent research attachments at University of Oxford and Nippon Institute of Technology, respectively. Yeap is a senior member of the IEEE and a member of the IET. He is also a Chartered Engineer registered with the UK Engineering Council and a Professional Engineer registered with the Board of Engineers Malaysia. He is currently an associate professor in Universiti Tunku Abdul Rahman. Throughout his career, Yeap has served in various administrative capacities, Science including the Head of Programme of Master of Engineering and the Head of Department of Electronic Engineering. Yeap's research areas of interests are in radio astronomy, electromagnetics, and microelectronics. He has published 74 journal papers, 39 conference proceedings, 7 books, and 13 book chapters. Yeap is the external examiner of Wawasan Open University. He is the editor in chief of the i-manager's *Journal on Digital Signal Processing*. Yeap has been given various awards that include the university teaching excellence award, 4 Kudos awards from Intel Microelectronics, and 19 research grants.